ELSEVIER

Clinical Neurophysiology 119 (2008) 1756–1770

www.elsevier.com/locate/clinph

Detection of focal epileptiform events in the EEG by spatio-temporal dipole clustering

Peter Van Hese[a,*], Bart Vanrumste[c,d], Hans Hallez[a], Grant J. Carroll[h], Kristl Vonck[b], Richard D. Jones[e,f,g,i], Philip J. Bones[e], Yves D'Asseler[a], Ignace Lemahieu[a]

[a] *Department of Electronics and Information Systems, Medical Image and Signal Processing, Ghent University-IBBT-IBiTech, De Pintelaan 185 Block B, B-9000 Ghent, Belgium*

[b] *Department of Neurology, Laboratory of Clinical and Experimental Neurophysiology, Ghent University Hospital, De Pintelaan 185, B-9000 Ghent, Belgium*

[c] *Department of Electrical Engineering (ESAT/SCD), Katholieke Universiteit Leuven, Kasteelpark Arenberg 10, B-3001 Leuven, Belgium*

[d] *Katholieke Hogeschool Kempen, Kleinhoefstraat 4, B-2440 Geel, Belgium*

[e] *Department of Electrical and Computer Engineering, University of Canterbury, Private Bag 4800, Christchurch, New Zealand*

[f] *Department of Medical Physics and Bioengineering, Christchurch Hospital, Private Bag 4710, Christchurch, New Zealand*

[g] *Department of Medicine, University of Otago (Christchurch), P.O. Box 4345, Christchurch, New Zealand*

[h] *Department of Neurology, Christchurch Hospital, Private Bag 4710, Christchurch, New Zealand*

[i] *Van der Veer Institute for Parkinson's and Brain Research, P.O. Box 2682, Christchurch, New Zealand*

Accepted 1 April 2008
Available online 21 May 2008

Abstract

Objective: Methods for the detection of epileptiform events can be broadly divided into two main categories: temporal detection methods that exploit the EEG's temporal characteristics, and spatial detection methods that base detection on the results of an implicit or explicit source analysis. We describe how the framework of a spatial detection method was extended to improve its performance by including temporal information. This results in a method that provides (i) automated localization of an epileptogenic focus and (ii) detection of *focal* epileptiform events in an EEG recording. For the detection, only one threshold value needs to be set.

Methods: The method comprises five consecutive steps: (1) dipole source analysis in a moving window, (2) automatic selection of focal brain activity, (3) dipole clustering to arrive at the identification of the epileptiform cluster, (4) derivation of a spatio-temporal template of the epileptiform activity, and (5) template matching. Routine EEG recordings from eight paediatric patients with focal epilepsy were labelled independently by two experts. The method was evaluated in terms of (i) ability to identify the epileptic focus, (ii) validity of the derived template, and (iii) detection performance. The clustering performance was evaluated using a leave-one-out cross validation. Detection performance was evaluated using Precision-Recall curves and compared to the performance of two temporal (mimetic and wavelet based) and one spatial (dipole analysis based) detection methods.

Results: The method succeeded in identifying the epileptogenic focus in seven of the eight recordings. For these recordings, the mean distance between the epileptic focus estimated by the method and the region indicated by the labelling of the experts was 8 mm. Except for two EEG recordings where the dipole clustering step failed, the derived template corresponded to the epileptiform activity marked by the experts. Over the eight EEGs, the method showed a mean sensitivity and selectivity of 92 and 77%, respectively.

Conclusions: The method allows automated localization of the epileptogenic focus and shows good agreement with the region indicated by the labelling of the experts. If the dipole clustering step is successful, the method allows a detection of the focal epileptiform events, and gave a detection performance comparable or better to that of the other methods.

Significance: The identification and quantification of epileptiform events is of considerable importance in the diagnosis of epilepsy. Our method allows the automatic identification of the epileptic focus, which is of value in epilepsy surgery. The method can also be used as an offline exploration tool for focal EEG activity, displaying the dipole clusters and corresponding time series.

* Corresponding author. Tel.: +32 9 240 4326; fax: +32 9 240 4159.
E-mail address: Peter.VanHese@UGent.be (P. Van Hese).

doi:10.1016/j.clinph.2008.04.009

Keywords: Detection of epileptiform events; Focal epileptiform activity; Paediatric patients; Focal epilepsy; Dipole clustering

1. Introduction

The detection of epileptiform events in the EEG has been a long-standing goal. Since the late '70s different approaches towards automatic detection have been proposed (see Frost (1985), Wilson and Emerson (2002) for a review). Typically, these detection methods are classified according to the signal processing technique(s) used: mimetic, linear predictive filtering, template matching, artificial neural networks, independent component analysis, etc. Alternatively, these detection methods can be broadly divided into two main categories: temporal detection methods that exploit the EEG's temporal characteristics, and spatial detection methods that base the detection on the results of an implicit or explicit source analysis.

Methods from the first category include mimetic approaches which perform a morphological analysis. Features related to the spike morphology such as the amplitude, sharpness and duration are derived by a wave and halfwave analysis (Gotman and Gloor, 1976; Dingle et al., 1993). Morphological features can also be derived using the discrete or continuous wavelet transformation (Goelz et al., 2000; Latka et al., 2003) or the Walsh transformation (Adjouadi et al., 2004; Adjouadi et al., 2005). Detection is accomplished by comparing the estimated features with some predefined thresholds typical for epileptiform discharges (Gotman and Gloor, 1976) or via an artificial neural network (Acir et al., 2005; Tzallas et al., 2006). All temporal detection methods are designed to be applied to one channel of the EEG, and thus do not take advantage of the information on the topography of the epileptiform events. To exploit the relationship between the different channels, these methods are typically applied to each channel individually and subsequently the detection results are combined. In its simplest form, a requirement is that one event should be found simultaneously on different channels (Black et al., 2000; Acir et al., 2005). An enhanced approach is to use an expert system to incorporate *a priori* knowledge on the expected field distribution (Glover et al., 1989; Dingle et al., 1993; James et al., 1999; Liu et al., 2002; Tzallas et al., 2006).

Spatial methods on the other hand assume a model of the underlying electrical activity and base the detection on the results of a source analysis. The advantage of this approach is that the relationship between the different channels is fully exploited. This information is included from the onset of the analysis, based on a physical model, rather than incorporated afterwards, more or less *ad-hoc*. The detection method in Kobayashi et al. (2002) is based on independent component analysis (ICA) and a dipole analysis of the ICA components. The method in Ossadtchi et al. (2004) is a method applied to MEG, based on source analysis using ICA and recursively applied and projected multiple signal classification (RAP-MUSIC). In Van Hoey (2000), Van Hoey et al. (2000) the detection is performed by searching for focal epileptiform activity using a principal component analysis (PCA) decomposition and a single dipole source model. However, in general, these spatial methods do not fully exploit the temporal information. The method by Van Hoey (2000), Van Hoey et al. (2000) does not put any restrictions on the waveform which makes the method useful for searching for any focal activity in the EEG but results in a low detection performance for epileptiform events, since it picks up activity that does not match typical epileptiform activity (Vanrumste et al., 2005).

In this paper we describe how the framework of the spatial detection method described in Van Hoey (2000), Van Hoey et al. (2000) can be extended to make use of the valuable temporal information in the EEG. This results in a method that provides (i) automated localization of an epileptogenic focus and (ii) detection of *focal* epileptiform events in an EEG recording. We have applied and evaluated our method on the EEG of eight paediatric patients with focal epilepsy.

2. Methods

2.1. EEG data

The data set consisted of eight routine EEG records (sampled at 256 Hz, 1–30 Hz band-pass filtered, 19 electrodes according to the international 10–20 standard, average referenced) from eight paediatric patients with focal epilepsy. The patients had an average age of 5.5 years (range 3–10 years). The patients were selected out of a pool of available data to include only paediatric patients. Each EEG record lasted 12–21 min (total duration: 2 h 10 min). All EEGs were recorded while patients were awake. EEGs were included only if they displayed at least one definite epileptiform event. Bad quality EEGs were excluded. There were no EKG artifacts. This data set was the same as that in Vanrumste et al. (2005).

The epileptiform events in each recording were labelled independently by two experienced electroencephalographers (G.C., K.V.) as definite or questionable. Both scorings were then used to construct a consensus labelling (*gold standard*) for evaluation of the detection methods. Table 1 lists a summary of the EEG records and the clinical findings for each patient.

Table 1
Summary of the EEG records and clinical findings for the eight paediatric patients for which EEG data was analysed in this study

Patient	Sex/age	Duration (m:s)	GC #d + #q	KV #d + #q	Consensus #d + #q	EEG summary	Brain scan summary
1	M/4	12:26	19 + 66	43 + 54	41 + 73	Parasagittal epileptiform discharges prominent from the left central region	Moderately extensive left-side infarction (MRI)
2	F/3	13:30	65 + 97	43 + 107	75 + 135	Diffuse excess of fast activity and frequent discharges mostly arising from the left occipital region	Diffuse hypoxic/ischaemic brain injury (CT)
3	F/4	14:19	6 + 92	114 + 219	67 + 268	Discharges predominantly from right parietal region, plus slower background from this region	No record
4	F/5	13:21	1 + 105	4 + 109	2 + 158	Right central and mid-temporal discharges with a slow background	Destructive white matter lesion in right frontal lobe (MRI)
5	M/5	20:52	96 + 88	52 + 154	106 + 111	Occipital sharp waves typical of benign occipital epilepsy	Normal (MRI)
6	M/6	13:35	16 + 159	30 + 119	44 + 150	Drug induced beta, right antero-temporal to mid-temporal sharp wave discharges	No record
7	M/7	20:53	7 + 31	7 + 29	9 + 30	Right centro-temporal sharp wave discharges	Normal (CT)
8	F/10	21:10	102 + 167	193 + 126	174 + 182	Slowing in right anterior quadrant and right frontal sharp spike and wave discharges	Right frontal lobe lesion (MRI)
Total		02:10:06	312 + 805	486 + 917	518 + 1107		

#d and #q are the number of definite and questionable epileptiform events, as labelled by two experts (G.C. and K.V.).

2.2. Spatio-temporal detection method

Our new method for detection of focal epileptiform events comprises five consecutive steps: (1) dipole source analysis of the EEG in a moving window, (2) selection of focal brain activity based on the source analysis results, (3) clustering of dipoles to identify an epileptiform cluster, (4) derivation of a spatio-temporal template of the epileptiform activity, and (5) template matching using the derived template to identify the epileptiform activity present in the EEG recording. A schematic overview of this method is depicted in Fig. 1.

The goal of the first two steps is to select sufficient time instances that represent the focal epileptiform activity we are interested in. The dipole clustering in the third step allows us to derive a spatio-temporal template of this activity. This template is used in the fourth and fifth steps to identify the occurrences of the activity in the EEG recording.

2.2.1. Dipole source analysis

The EEG $\mathbf{X} \in \mathbb{R}^{m\times n}$ (m electrodes, n time samples) is analysed in a moving window with length $L = 64$ (250 ms) and step size $S = 6$ (25 ms). For each window k, centred around the time instance $t_k = (k-1)S + L/2$, the EEG segment $\mathbf{W}_k = \mathbf{X}(:, t_k \pm L/2) \in \mathbb{R}^{m\times L}$ is decomposed by a principal component analysis (PCA), using a singular value decomposition (SVD): $\mathbf{W}_k = \mathbf{U}_k\Sigma_k\mathbf{V}_k^{\mathrm{T}}$, and the first left eigenvector (which represents the potential topography of the first principal component) is analysed using a dipole model by minimizing the following cost function:

$$\mathrm{RRE}_k = ||\mathbf{U}_k(:,1) - \mathbf{L}(\mathbf{r}_k)d_k\mathbf{e}_k||_2^2 \tag{2.1}$$

with $\mathbf{r}_k$ the dipole position, $\mathbf{d}_k = d_k\mathbf{e}_k$ the dipole components (dipole intensity and orientation), $\mathbf{L} \in \mathbb{R}^{m\times 3}$ the lead field matrix which relates the dipole parameters to the surface potentials, and RRE_k the relative residual energy (the fraction of the energy which cannot be explained by a dipolar field). For the minimization of the cost function, we chose the Nelder–Mead simplex algorithm (Nelder and Mead, 1965), because of its relative simplicity. A three-shell spherical head model (Salu et al., 1990) was used with radii equal to 8.0, 8.5 and 9.2 cm for the brain, skull and scalp compartment, respectively, and a soft tissue to skull conductivity ratio of 16 (Oostendorp et al., 2000).

For each window k, we defined S_k as the fraction of the energy of the first principal component:

$$S_k = \frac{\sigma_{1k}^2}{\sum_{i=1}^{m}\sigma_{ik}^2} \tag{2.2}$$

Each EEG segment $\mathbf{W}_k$ is thus modelled as

$$\begin{aligned}\mathbf{W}_k &\cong \mathbf{U}_k(:,1)\sigma_{1k}\mathbf{V}_k(:,1)^{\mathrm{T}} \\ &\cong \mathbf{L}(\mathbf{r}_k)d_k\mathbf{e}_k\sigma_{1k}\mathbf{V}_k(:,1)^{\mathrm{T}},\end{aligned} \tag{2.3}$$

where the approximation is more accurate for high S_k and low RRE_k. The dipole time series are contained in the first right eigenvector $\mathbf{V}_k(:,1)^{\mathrm{T}} \in \mathbb{R}^{1\times L}$. The time series $\mathbf{y}_k \in \mathbb{R}^{1\times 2L}$ of the active source in a neighbourhood of length $2L$ centred around the k^{th} window can be found by a spatial filter using the first left eigenvector as a weight vector: $\mathbf{y}_k = \mathbf{U}_k(:,1)^{\mathrm{T}}\mathbf{X}(:, t_k \pm L)$. Due to the orthogonality constraint of the SVD, *inside* the analysis window, $\mathbf{y}_k \equiv \sigma_{1k}\mathbf{V}_k(:,1)^{\mathrm{T}}$.

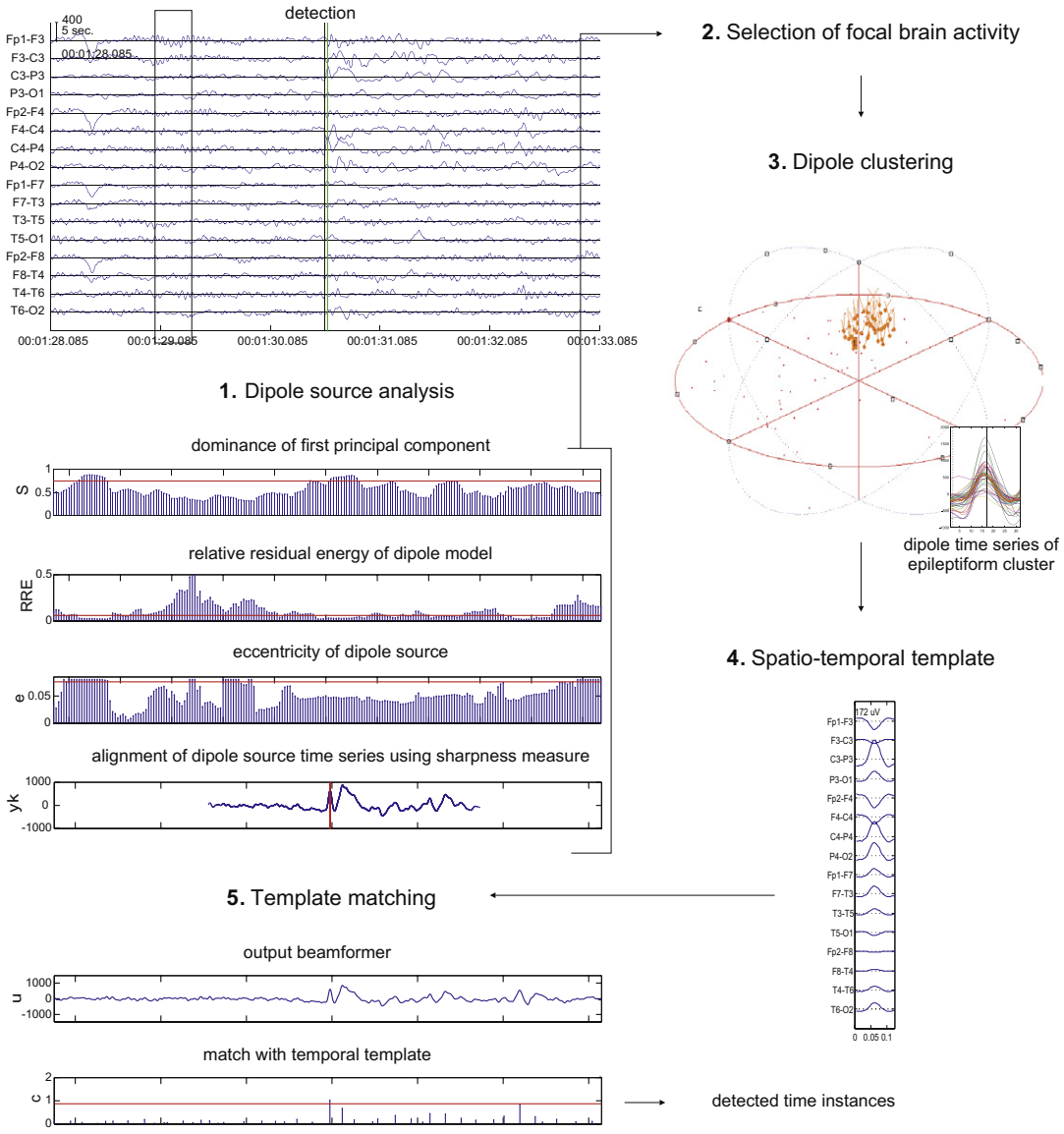

Fig. 1. A schematic overview of the detection method. The method comprises five consecutive steps: (1) dipole source analysis of the EEG in a moving window, (2) selection of focal brain activity based on the source analysis results, (3) clustering of dipoles to identify an epileptiform cluster, (4) derivation of a spatio-temporal template of the epileptiform activity, and (5) template matching using the derived template to identify the epileptiform activity present in the EEG recording.

2.2.2. Selection of focal brain activity

Focal brain activity is identified by selecting all windows k that fulfil the criteria (i) $S_k > \theta_S$, (ii) $\mathrm{RRE}_k < \theta_{\mathrm{RRE}}$, and (iii) $||\mathbf{r}_k||_2 < \theta_e$. The first criterion ensures the presence of a single dominant source. The second criterion confirms the detection of a source characterized by a dipolar field and, hence a focal source. Nevertheless, it is possible to obtain low RRE values for spatially extended sources (Hara et al., 1999), and, therefore, a low RRE value is a necessary but not sufficient condition. The third criterion places a restriction on the dipole eccentricity so that only physiological meaningful dipole sources are retained and certain EEG artifacts are removed (Flanagan et al., 2003).

The threshold θ_e was set to $0.95 * 8.0$ cm, corresponding to the outer limit of the cortex, since we use a three-shell spherical head model with an inner radius of 8.0 cm. θ_S and θ_{RRE} are two free parameters of the method still to be determined.

Each selected window is characterized by a dipole position $\mathbf{r}_k$, orientation $\mathbf{e}_k$, and time series $\mathbf{y}_k$. However, before these parameters can be used in the dipole clustering step of the algorithm, three issues need to be resolved. First, to allow the construction of a temporal template, an alignment of the dipole time series is necessary. Also, we found that for some epileptiform events consisting of a spike-and-wave complex the parameter S used in the selection step of the method obtains its highest values *at the wave* of the epileptiform events, rather than at the spike. So some of the selected windows were positioned on the wave following the spike, rather than on the spike. Since

we want to extract the temporal waveform of the spike, we need to look at the time series in a small neighbourhood around the selected windows. Next, since the dipole orientation can be flipped by changing the sign of the dipole time series (and vice versa), without affecting the model in Eq. (2.3), there is a sign ambiguity in the dipole orientation and dipole time series. Finally, because we use overlapping windows in the analysis, typically, a single event results in the selection of a number of consecutive segments which will have to be grouped into one selected representative segment.

See Fig. 2 for an illustration of the time series obtained in consecutive selected windows.

The alignment problem was resolved by calculating the sharpness $\mathbf{s}_k$ of the time series $\mathbf{y}_k$ and aligning the time series at the point τ_k of maximal sharpness magnitude: $\tau_k = \arg\max|\mathbf{s}_k|$. The sharpness was calculated by twice applying a linear regression filter with a width of 20 ms $(A = 2) : \mathbf{a}_k(n) = \sum_{i=-A}^{A} i\mathbf{y}_k(n+i), \mathbf{s}_k(n) = \sum_{i=-A}^{A} i\mathbf{a}_k(n+i)$. The sign ambiguity was resolved by forcing the sharpness to be negative at τ_k (thus forcing the spike to exhibit a local maximum at this point). Selected (consecutive) windows for which the difference between their associated time instances τ_k was smaller then 125 ms were replaced by the selected window for which its centre position was closest to its associated time instance τ_k.

Choosing a window of length $L_t = 125$ ms centred around τ_k, we obtain a set of selected EEG segments, each representing focal brain activity characterized by a dipole position $\mathbf{r}_k$, dipole orientation $\mathbf{e}'_k$, and (aligned) time series $\mathbf{y}'_k$:

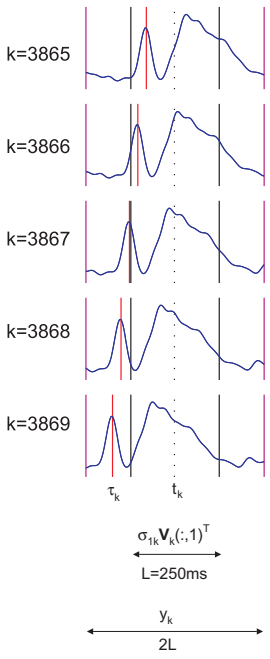

Fig. 2. An illustration of the time series obtained in consecutive selected windows. The borders of the moving analysis window are indicated with black vertical lines. The red vertical line indicates the point of maximal sharpness magnitude. (For interpretation of the references to colour in this figure legend, the reader is referred to the web version of this paper.)

$$\begin{aligned}\mathbf{X}(\tau_k \pm L_t/2) &\cong \mathbf{L}(\mathbf{r}_k) d_k \mathbf{e}_k \mathbf{y}_k(\tau_k \pm L_t/2) \\ &= \mathbf{L}(\mathbf{r}_k)(\gamma \mathbf{e}_k)(\gamma d_k \mathbf{y}_k(\tau_k \pm L_t/2)) \\ &= \mathbf{L}(\mathbf{r}_k)\mathbf{e}'_k\mathbf{y}'_k \end{aligned} \tag{2.4}$$

with $\gamma = \text{sign}(-\mathbf{s}_k(\tau_k))$.

2.2.3. Spatio-temporal dipole clustering

The set of dipole positions $\mathbf{r}_k$ and orientations $\mathbf{e}'_k$ is clustered using a sequential clustering algorithm (Theodoridis and Koutroumbas, 1999), as used in Ossadtchi et al. (2004).

First, we calculate a dissimilarity matrix $\mathbf{Y}_r$ which contains the Euclidean distances between each pair of dipole position vectors $\mathbf{r}_i$ and $\mathbf{r}_j : \mathbf{Y}_r(i,j) = ||\mathbf{r}_i - \mathbf{r}_j||_2$. The first cluster is found by choosing the row i_1 for which $\sum_j I(\mathbf{Y}_r(i_1, j) < \delta_r)$ is maximal, with $I(\cdot)$ the indicator function $(I(\text{true}) = 1, I(\text{false}) = 0)$ and δ_r a preset threshold which determines the maximum radius of the dipole clusters. The first spatial cluster is the set of dipoles $I_1 = \{j : \mathbf{Y}_r(i_1, j) < \delta_r\}$ which are within a distance δ_r of the centroid i_1. The entries of the distance matrix corresponding to this set are removed and the procedure is repeated until the remaining clusters contain less then $N_{\min}$ dipoles, with $N_{\min}$ another preset threshold.

Next, each spatial cluster is subdivided into smaller clusters using the same procedure as above, but now with a dissimilarity matrix $\mathbf{Y}_e = \text{acos}(\mathbf{e}_i'^T \mathbf{e}'_j)$ containing the angles between each pair of dipole orientation vectors $\mathbf{e}'_i$ and $\mathbf{e}'_j$, and setting a threshold δ_e.

As a result, we obtain clusters of similar dipole position and orientation vectors. Similarly, each cluster could be subdivided using a dissimilarity matrix containing the Euclidean distances between the time series $\mathbf{y}'_k$. However, for our data the time series within each cluster already showed similar waveforms and no further clustering was needed.

For all EEG records, we set $N_{\min} = 10$ as the minimum number of required dipoles in one cluster. δ_r and δ_e are free parameters of the method that remain to be determined (see Section 2.3.4).

2.2.4. Spatio-temporal template

If more than one cluster is found, the cluster with the maximum sharpness magnitude at the peak of the normalized average of the time series corresponding to the dipoles in that cluster is assumed to correspond to the epileptiform region in the brain, and termed 'epileptiform cluster':

$$I_{\text{epi}} = \arg\max_{I_i} \left| \text{sharpness}\left(\frac{E\left[\mathbf{y}'_j\right]}{\left\|E\left[\mathbf{y}'_j\right]\right\|_2} \right) \right|, \quad j \in I_i, \tag{2.5}$$

with sharpness being the sharpness at the peak of the time series as calculated in Section 2.2.2. See Fig. 3 for an illustration of this selection criterion. A spatio-temporal template $\mathbf{T} \in \mathbb{R}^{m \times L_t}$ for activity from the epileptiform cluster was constructed using a dipole model,

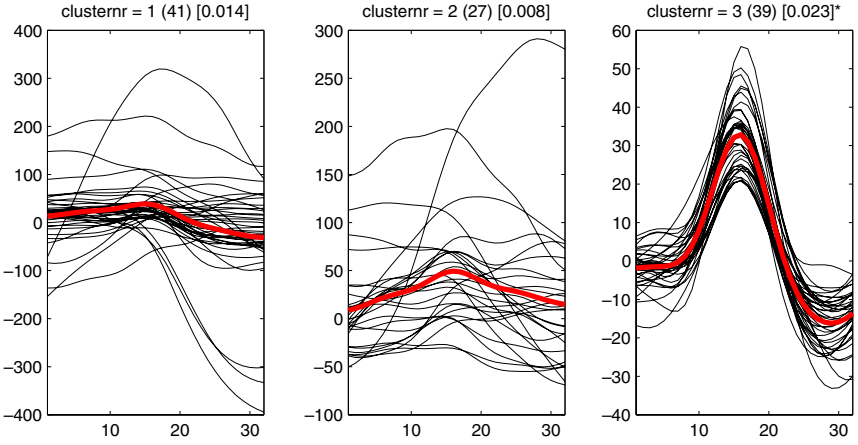

Fig. 3. The dipole time series for the three clusters found for EEG record 5. The red bold line is the average time series per cluster. The first two clusters show no typical epileptiform time series, while the third cluster reveals a clear epileptiform pattern. The third cluster was selected by the method as the epileptiform cluster because, of all three clusters, it has the largest sharpness magnitude at the peak of the normalized average time series (sharpness magnitude values are shown between square brackets). (For interpretation of the references to colour in this figure legend, the reader is referred to the web version of this paper.)

with the dipole position, orientation, and time series parameters equal to the mean of the dipole position, orientation, and time series parameters of the epileptiform cluster:

$$\mathbf{v}_T = \mathbf{L}(\mathbf{r}_T)\mathbf{e}_T$$
$$\mathbf{T} = \mathbf{v}_T\mathbf{y}_T \tag{2.6}$$

with $\mathbf{r}_T = E[\mathbf{r}_j], \mathbf{e}_T = E[\mathbf{e}'_j], \mathbf{y}_T = E[\mathbf{y}'_j], j \in I_{\text{epi}}$.

2.2.5. Template matching

In the final step of the algorithm, the signal $\mathbf{u} \in \mathbb{R}^{1\times n}$ originating from the position of the epileptiform cluster is monitored using a quiescent beamformer (Van Veen and Buckley, 1988), i.e., using a weight vector equal to $\mathbf{w}_Q = \mathbf{v}_T(\mathbf{v}_T^{\mathrm{T}}\mathbf{v}_T)^{-1} : \mathbf{u} = \mathbf{w}_Q^{\mathrm{T}}\mathbf{X}$. A detection is made for those time instances τ were the match $c(\tau) = \mathbf{u}(\tau \pm L_T/2)^{\mathrm{T}}\mathbf{y}_T/||\mathbf{y}_T||_2^2$ exhibits a local maximum and exceeds a detection threshold θ_c. Both $\mathbf{u}$ and $\mathbf{y}_t$ were zero-meaned to calculate $c(\tau)$. The match $c(\tau)$ is normalized so that $c(\tau)$ equals 1 for an epileptiform event in the EEG whose time series has the same norm as that of the template time series $\mathbf{y}_T$.

2.3. Evaluation of the spatio-temporal detection method

2.3.1. Localization of epileptic focus

To evaluate the localization results of the proposed method, the epileptiform events in the EEG labelled as definite according to the consensus scoring, were subjected to a dipole analysis. A window of $L_t = 125$ ms was centred around each time instance in the EEG marked as definite, and dipole parameters were fitted to the first principal component of this segment (using a three-shell spherical head model, radii 8.0, 8.5 and 9.2 cm, soft tissue to skull conductivity ratio of 16). Next, the point of highest density of the dipole location vectors was determined using the clustering procedure outlined in 2.2.3, with $\delta_r = 4.0$ cm and $N_{\min} = 1$. The mean of all dipoles in a sphere with radius 1.5 cm around the centroid of the first cluster served as the centre of a spherical region of definites (ROD) with radius 1.5 cm, indicating the epileptic focus (the value of 1.5 cm is not crucial here and is merely for visualization). To assess the concurrence of the epileptiform cluster with this ROD, the Eucledian distance d between the centre of the ROD and the mean of all dipole position vectors in the epileptiform cluster was calculated.

2.3.2. Template

The validity of the template was evaluated by comparing the template $\mathbf{T}$ with $\mathbf{V}_{\text{def}}$, the mean of all EEG segments whose dipole position vector lies inside the constructed ROD, using the error measure

$$\text{RRE} = \frac{\left\|\mathbf{V}_{\text{def}} - a_{\text{opt}}\mathbf{T}\right\|_F^2}{\left\|\mathbf{V}_{\text{def}}\right\|_F^2}, \tag{2.7}$$

with $a_{\text{opt}} = \sum_{ij}\mathbf{V}_{\text{def}}(i,j)\mathbf{T}(i,j)/\|\mathbf{V}_{\text{def}}\|_F^2$, and $\|\cdot\|_{\text{F}}$ the Frobenius norm.

2.3.3. Detection performance

In the following paragraphs, we describe three detection methods that served as a reference in the evaluation of the detection performance of the new detection method. The first two methods are temporal detection methods (mimetic and wavelet) which perform the detection on a single EEG channel (that has to be selected beforehand). The third method is a spatial detection method in which the detection is based on the results of dipole analysis in a moving window.

2.3.3.1. Mimetic detection method. This method is a basic temporal detection method, similar to the first step found in most mimetic algorithms (Gotman and Gloor, 1976; Glover et al., 1989; Dingle et al., 1993). The EEG is

divided into segments and sequences according to rules described in Gotman and Gloor (1976). Combinations of consecutive segments and sequences are termed halfwaves, and for each wave (a wave consists of two contiguous halfwaves) and its constituent halfwaves, the duration, amplitude, and sharpness at the top, are calculated according to the procedure described in Dingle et al. (1993).

A detection is made if all parameters exceed preset thresholds. In our implementation we chose to use only the amplitude and sharpness parameters, because (i) these parameters are the most important in characterizing an epileptiform waveform (Wilson et al., 1996) and (ii) we wanted to have a basic method as a reference. Note that due to the way waves and halfwaves are determined (via the rules adhered to in the decomposition of the EEG), the duration of the epileptiform activity is implicitly taken into consideration.

2.3.3.2. Wavelet detection method. This method is wavelet based as used by Latka et al. (2003). The algorithm is founded on the behaviour of the wavelet power spectrum of the EEG signal across scales (and thus not only on its values). The EEG is analysed in a moving window (length 5 s, overlap 1 s) by the continuous wavelet transform using the Mexican hat wavelet. To reduce dependence on the amplitude of the EEG, the wavelet power is normalized by the variance σ^2 of the EEG signal in the window being analysed: $w_a(n) = W_a^2(n)/\sigma^2$, with $W_a(n)$ the continuous wavelet transform of the EEG at time index n, and scale a. The square of the normalized wavelet power w_a^2 is observed in three different scales, and an epileptic spike is identified at time instance i if all of the following criteria are met: (i) $w_7^2(i) > w_{20}^2(i)$, i.e., the square of the normalized wavelet power decreases from scale 7 to scale 20, (ii) $w_7^2(i) > T_1$, and (iii) $w_3^2(i) > T_2$, with T_1 and T_2 two preset threshold values.

2.3.3.3. Dipole analysis detection method. This method is spatially based via the results of a dipole analysis and was proposed by Van Hoey (2000), Van Hoey et al. (2000). The EEG is analysed in a moving window (length 250 ms, step size 25 ms). In each window, the first principal component (obtained using a singular value decomposition (SVD)) is analysed using a fixed dipole model (three-shell spherical head model, radii 8.0, 8.5 and 9.2 cm, soft tissue to skull conductivity ratio of 16). A detection is made if (i) the fraction of the energy of the first principal component S is above a threshold θ_S, and (ii) the relative residual energy (RRE) of the dipole model drops below a threshold θ_{RRE}.

This method imposes no constraints on the waveform of the detected EEG signal. The underlying assumption is that the epileptiform activity is generated by a single focal source. The first criterion ensures the presence of a single dominant source. The second criterion confirms the detection of a source characterized by a dipolar field and, hence a focal source.

Table 2
Rules for the construction of a consensus labelling, given the dichotomous labelling (d, definite; q, questionable; –, no matching event) of two experts

Expert 1	d	d	q	q	d	q	–	–
Expert 2	d	q	d	q	–	–	d	q
Consensus	d	d	d	q	q	q	q	q

2.3.3.4. Evaluation measures. To evaluate the performance of the detection method(s), we calculated sensitivity and selectivity values. Sensitivity (or recall) is defined as the ratio between the number of TP (true positives) and the number of TP and FN (false negatives). Selectivity (or precision) is the ratio between the number of TP and the number of TP and FP (false positives).

Given the labelling of the two experts, Table 2 shows how to derive the *consensus labelling*. An event marked by the first expert is considered to match an event marked by the second expert, if the time difference between these two events is smaller than 250 ms. Consecutive markings are counted as one, if their time instances fall within a time window of 500 ms. Because of labelling into two categories (definite and questionable), additional rules were required to agree on the definition of the TP, FP and FN. Given the consensus labelling and the results of the detection method, Table 3 shows the rules we adhered to for the comparison of the different markings.

Each detection method was evaluated by comparing the detection result with the consensus labelling. For each method we constructed a precision-recall curve (PR-curve), which depicts the trade-off between sensitivity and selectivity, for different values of the detection parameter(s). As a summary of the PR-curve, we tabulated the sensitivity and selectivity values of the working point M, defined as the point on the PR-curve closest to the optimal point (1.00, 1.00). This point M was chosen over the intercept of the PR-curve with the line of equal sensitivity and selectivity, because for some EEG records equal sensitivity and selectivity could not be obtained due to the influence of artifacts on the detection performance of the particular detection method.

Table 3
Rules for the assignment into TP (true positives), FP (false positives) and FN (false negatives) (ni, not included for the calculation of sensitivity and selectivity), given a consensus labelling and the set of events marked by a detection method (d, definite; q, questionable; D, detected; –, no matching event)

Consensus	d	d	q	q	–
Detector	D	–	D	–	D
Event	TP	FN	TP	ni	FP

2.3.4. Leave-one-out cross validation

The method requires the selection of four free parameters, i.e., $\theta_S, \theta_{\mathrm{RRE}}, \delta_r$ and δ_e. These parameters control the derivation of the spatio-temporal template: θ_S and θ_{RRE} control n (the total number of windows selected is in percentage, relative to the total number of windows), the total number of windows selected (after grouping), while δ_r and δ_e control the formation of the epileptiform cluster used for the construction of the template. To obtain a good detection performance, these parameters should be chosen so that the derived template matches, as closely as possible, the epileptiform activity we are interested in. Optimal parameter values can thus be set by minimizing the error measure RRE (Eq. 2.7) as a function of these parameters.

To obtain a fair estimate of the performance of the method, we used a leave-one-out cross validation. This is a well-established method for estimating the performance of a method when the available data set is too small to allow a separate training and test set (Theodoridis and Koutroumbas, 1999). If the EEGs used are representative of the population, a leave-one-out cross validation provides a sound estimate of the performance that would be achieved with a separate test set.

Seven out of eight EEG records were used for training (training set), and the remaining EEG was used for testing (test set). This procedure was repeated eight times so that all EEGs were used once for testing. Optimal parameters per EEG were obtained by minimizing the error measure RRE as a function of $\theta_S, \theta_{\mathrm{RRE}}, \delta_r$ and δ_e. The parameter values were varied as follows (using the notation minimum : step size : maximum): $\theta_S = 0 : 0.01 : 1, \theta_{\mathrm{RRE}} = 0 : 0.005 : 0.06, \delta_r = 1 : 0.1 : 2.5$ cm, $\delta_e = 0 : 5 : 45°, n = 0 : 01 : 0.55\%$. Optimal values of θ_S and θ_{RRE} result in n^* total number of selected windows. If θ_{RRE} is kept constant, there is a one-to-one relationship between θ_S and n.

Optimal parameters over the training set were obtained by taking the average of the individual optimal parameter values $n^*, \theta_{\mathrm{RRE}}, \delta_r$ and δ_e of each EEG of the training set and setting θ_S so that the derived optimal number of windows were selected for the test EEG. Averaging over the individual values of n^* was preferred to averaging over the individual θ_S values as the latter shows a greater inter-subject variability, and the goal of the first step of the method is to selected sufficient time instances of the focal epileptiform activity of interest. The optimal parameters obtained using the training set were then used for the test EEG.

Table 4
Summary of the main findings of the evaluation of the method

EEG	Dipole clustering	Localization of epileptic focus d (cm)	Template RRE	Detection performance
1	Ok	0.1	0.22	Ok
2	Ok	0.5	0.55[a]	Ok
3	Ok	0.8	0.21	Ok
4	Ok	0.6	0.13	Ok
5	Ok	0.6	0.06	Ok
6	Ok	1.0	0.50[a]	Ok
7	Nok[b]	7.8	0.85	Nok[c]
8	ok[d]	1.9	0.98, Nok[e]	Nok[f]

[a] Good template for detection, relatively high RRE value due to background EEG activity not related to the epileptiform events.
[b] Clustering failed.
[c] No valid template could be derived because clustering failed.
[d] Widespread activity; no typical epileptiform time series revealed; epileptiform cluster pointed to correct brain region.
[e] Widespread activity that cannot be modelled using a single dipole model.
[f] Low performance due to an inadequate template; widespread activity.

Table 5
Per EEG record, the individual optimal parameter values for the derivation of the spatio-temporal template

EEG	θ_S	θ_{RRE}	δ_r (cm)	δ_e (°)	n^*	RRE
1	0.72	0.050	1.5	30	0.46	0.15
2	0.63	0.025	2.5	10	0.38	0.51
3	0.65	0.035	1.3	30	0.53	0.13
4	0.76	0.030	2.1	5	0.51	0.12
5	0.75	0.030	1.8	20	0.31	0.06
6	0.41	0.025	2.0	45	0.21	0.39
7	0.67	0.035	2.1	20	0.44	0.40
8	0.80	0.025	2.2	35	0.50	0.72

The last two columns show the total number of windows selected (in percentage) and the RRE value obtained with these parameter values.
[*] These numbers are expressed in percentages (%).

3. Results

Table 4 summarizes the main findings regarding the evaluation of the method (dipole clustering, localization of epileptiform focus, template and detection performance).

3.1. Leave-one-out cross validation

Table 5 shows the individual optimal parameter values per EEG obtained by minimizing RRE. Table 6 lists, per test EEG, the optimal parameter values obtained using the training set, as well as the RRE value obtained for that particular test record. Obviously, the RRE value obtained

Table 6
Parameter values for the derivation of the spatio-temporal template obtained in the leave-one-out cross validation setup

EEG	n^*	θ_{RRE}	δ_r (cm)	δ_e (°)	θ_S	RRE
1	0.41	0.029	2.0	24	0.57	0.22
2	0.42	0.033	1.9	26	0.69	0.55
3	0.40	0.031	2.0	24	0.66	0.21
4	0.40	0.032	1.9	27	0.79	0.13
5	0.43	0.032	2.0	25	0.70	0.06
6	0.45	0.033	1.9	21	0.38	0.50
7	0.41	0.031	1.9	25	0.65	0.85
8	0.41	0.033	1.9	23	0.84	0.98

Values for each test EEG are obtained by taking the average of the individual optimal parameters over all EEGs in the training set (i.e., all records excluding the test EEG). The last column shows the RRE value obtained for the test EEG for these parameter values.
[*] These numbers are expressed in percentages (%).

for each test EEG is lower then the corresponding RRE value obtained with the individual optimal parameters. All results shown in the following sections are with the parameters for each EEG set as listed in Table 6.

3.2. Dipole clustering

Fig. 4 shows the results of the clustering of the dipole position and orientation vectors representing focal brain activity. The three leftmost figures in each row show the dipoles in a frontal, top and side view, respectively, to give a better understanding of the 3D locations of the dipoles in the spherical head model. Each cluster is indicated by a circle with a radius of 15 mm and its centre equal to the mean of all dipole position vectors of that cluster. The epileptiform cluster is shown in red, while other clusters (if any) are plotted in blue. The rightmost figure in each row shows the dipole time series of the epileptiform cluster. The red bold line is the average time series. From this figure we can appreciate that the method succeeded, except for record 7, in forming clusters of dipoles with similar position and orientation vectors representing the focal brain activity in the recording, and extracting the corresponding time series. Isolated or randomly scattered dipole sources are not grouped into a cluster.

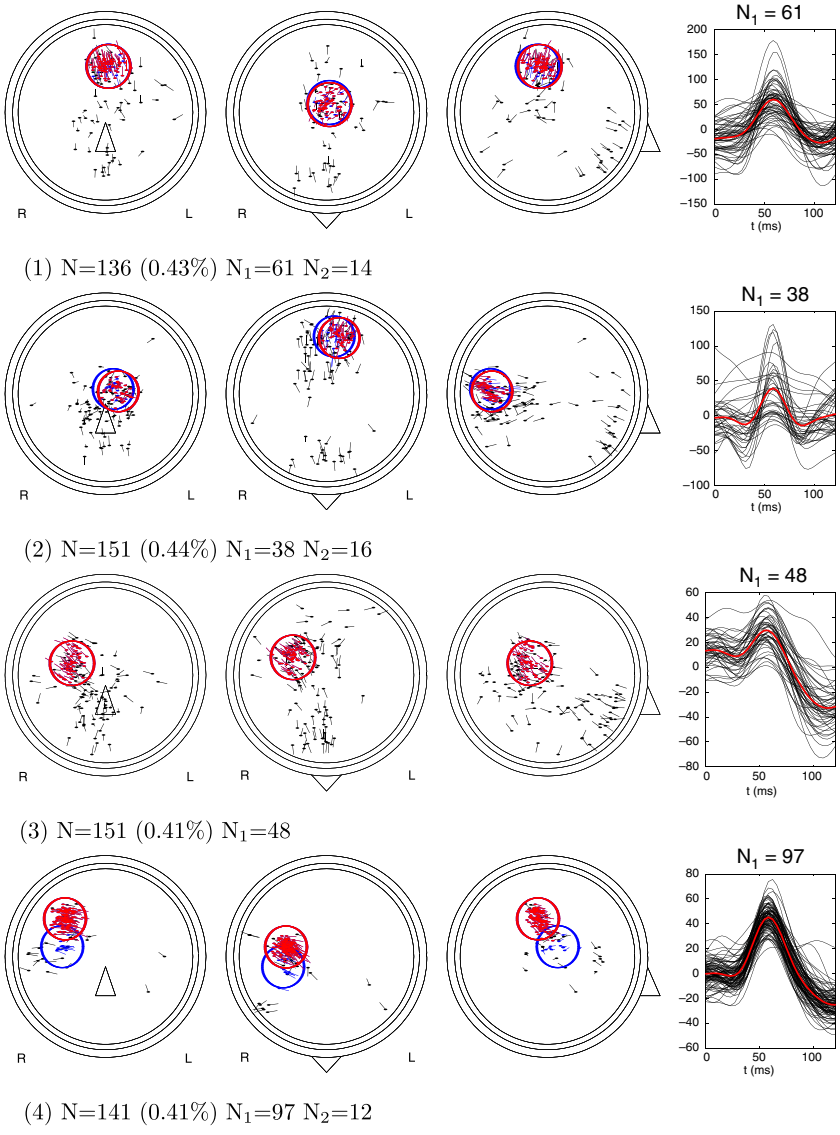

Fig. 4. Results of the clustering of the dipole position and orientation vectors representing focal brain activity. The three leftmost figures show the dipoles in a frontal, top and side view, respectively. Each found cluster is indicated by a circle with a radius of 15 mm and its centre equal to the mean of all dipole positions of that cluster. The epileptiform cluster is shown in red, while other clusters (if any) are plotted in blue. N denotes the total number of selected windows (and hence dipoles). N_i denotes the number of dipoles in cluster i. The rightmost figures show the dipole time series of the epileptiform cluster. The red bold line is the average time series. For all EEG records, the method succeeded in identifying the epileptiform cluster, except for EEG record 7. For EEG record 8, the method could not identify typical epileptiform time series due to widespread activity, although the epileptiform cluster found pointed to the correct brain region. (For interpretation of the references to colour in this figure legend, the reader is referred to the web version of this paper.)

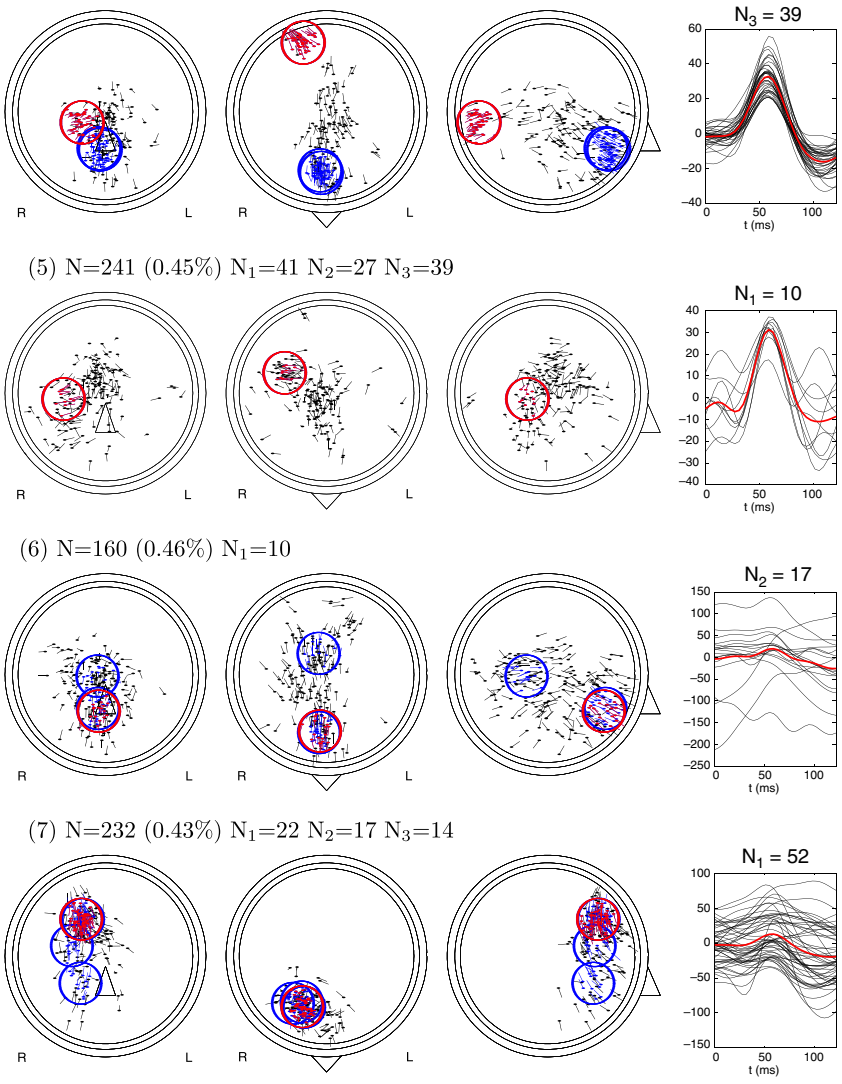

Fig. 4 (*continued*)

For record 5, the method found three clusters. Fig. 3 displays the dipole time series corresponding to these three clusters. From this figure the epileptiform cluster can easily be identified, as the first two clusters show no typical epileptiform time series, while the third cluster reveals a clear epileptiform pattern. The method automatically determined the third cluster as the epileptiform cluster because it has the largest sharpness magnitude at the peak of the normalized average time series (sharpness magnitude values are indicated between square brackets). Also for the other records where the method found more than one cluster, it correctly identified the epileptiform cluster by examining the sharpness at the peak of the averaged dipole time series per cluster.

For record 7, the method fails as no cluster was found that corresponded to the epileptiform activity. The epileptiform activity could only be found by manually lowering the parameter θ_S. When sufficient windows were selected, the method could identify the epileptiform cluster. For record 8, the method formed four clusters, but none of these revealed a typical epileptiform time series. The clinical summary of this EEG states that "throughout the recording there are right frontal sharp, spike and slow wave discharges. These may be confined to the right frontal quadrant or may spread to involve the whole of the right hemisphere and occasionally become incompletely generalized." This widespread activity cannot adequately be captured by the method, as the method explicitly relies on a dipole model representing focal brain activity. This is also reflected in the high RRE value of 0.98 (and for parameters optimal for this EEG it is still 0.72, see Tables 5 and 6). However, the clusters formed by the method do point to the region in the brain involved in the epileptiform activity.

3.3. Localization of epileptic focus

Fig. 5 shows the comparison of the epileptiform cluster with the dipole analysis results of the definite epileptiform

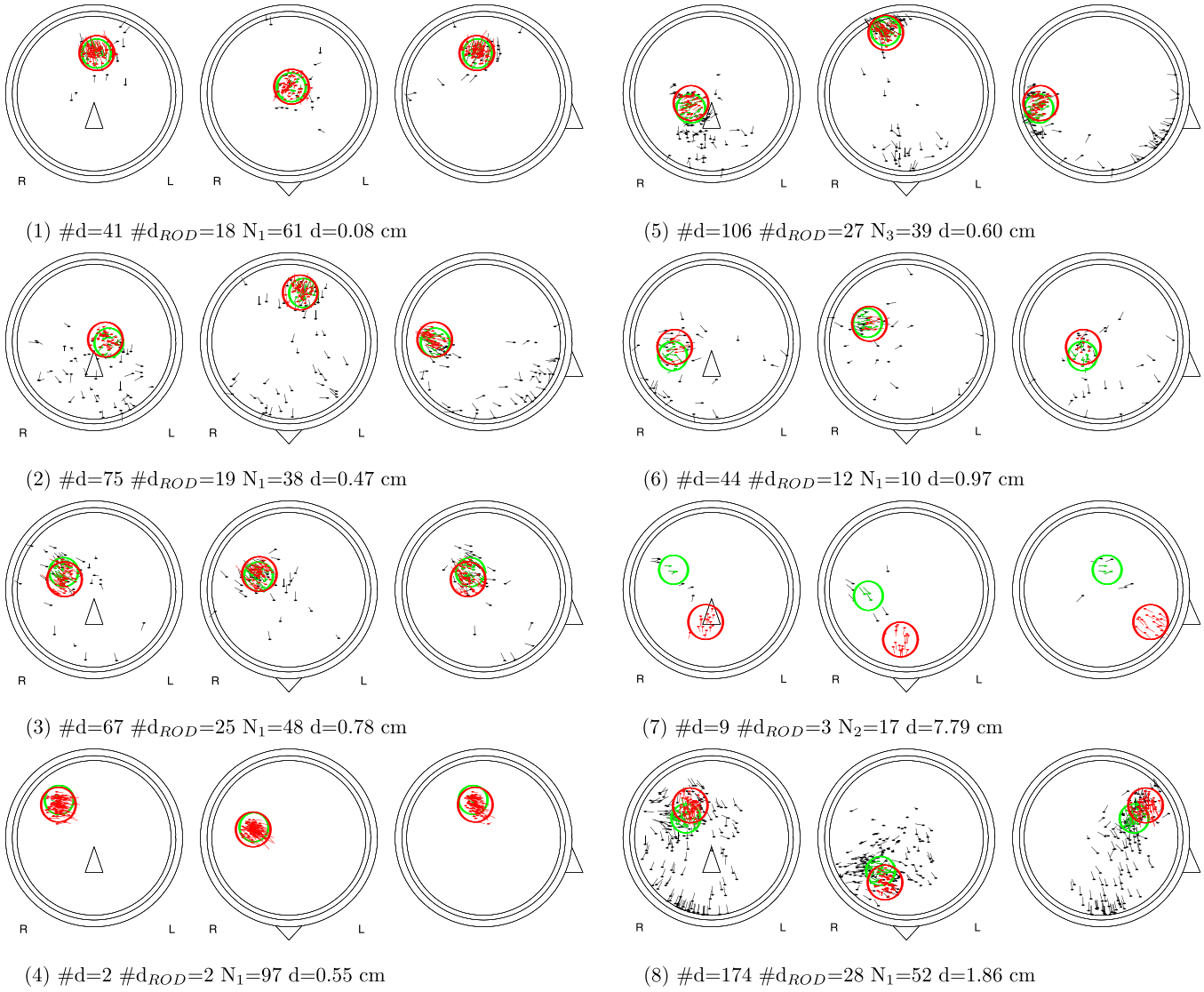

Fig. 5. Comparison of the epileptiform cluster with the dipole analysis results of the definite epileptiform events. The figures show all dipoles corresponding to the definite epileptiform events in the consensus labelling, in a frontal, top and side view, respectively. The region of definites (ROD) was established as the region of highest dipole position vector density. The ROD is indicated by a green circle of radius 1.5 cm. Superimposed on this plot are the dipoles of the epileptiform cluster (in red), indicated by red circle with radius 15 mm. #d denotes the number of definite epileptiform events in the consensus labelling, $\#d_{ROD}$ the number of dipoles in the ROD, N_i the number of dipoles in the epileptiform cluster and d is the Euclidean distance between the centre of the ROD and the centre of the epileptiform cluster. The results show a good concurrence of the epileptiform cluster with the ROD, with an average distance of 8 mm (leaving out EEG record 7 for which the clustering failed). Note the systematic shift between both regions. (For interpretation of the references to colour in this figure legend, the reader is referred to the web version of this paper.)

events in the consensus labelling. The figure shows all dipoles corresponding to the definite epileptiform events in a frontal, top and side view, respectively. The region of definites (ROD) is indicated by a green circle of radius 15 mm. Superimposed on this plot are the dipoles of the epileptiform cluster (in red), indicated by a red circle with radius 15 mm. From this figure we can appreciate the concurrence of the epileptiform cluster with the ROD. If we leave out record 7 (for which the clustering fails), the mean distance between the two regions was 8 mm, showing a good agreement.

For record 7 no agreement with the ROD was found. For record 8, as already discussed, there is a large scatter of the dipoles corresponding to the epileptiform events. This widespread activity makes it difficult to speak of a ROD. Nonetheless, the epileptiform cluster is found in the frontal region, in accordance with the clinical findings of this patient.

Note that for the construction of the ROD, dipole analysis was performed with the dipole analysis window centred on the peak of the spike of the definite epileptiform events in the consensus labelling. The detection method on the other hand returns dipole positions from a dipole analysis of automatically selected windows. Although the dipole time series are aligned at the point of maximal sharpness magnitude prior to the clustering

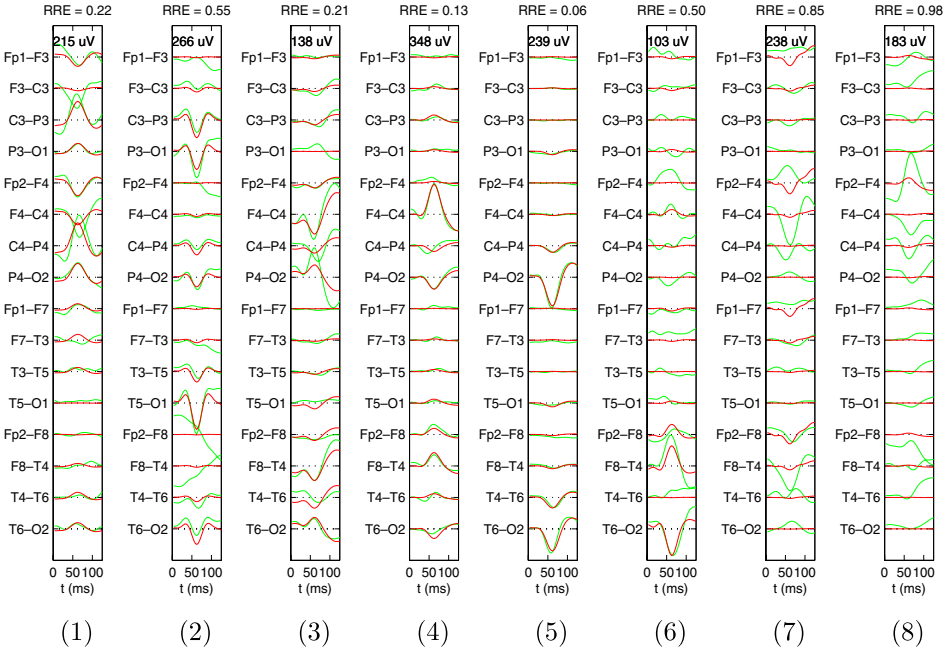

Fig. 6. Comparison of the spatio-temporal template **T** (in red) with $\mathbf{V}_{\text{def}}$, the mean of all EEG segments that correspond to the definite epileptiform events (in green). The results indicate a good agreement with a low value of RRE, except for EEG records 7 (clustering failed) and 8 (widespread activity). For EEG records 2 and 6 we find a relatively high value of RRE due to background EEG activity not related to the epileptiform events (channels Fp2-F8 and F8-T4 for EEG record 2, and channel Fp2-F4 for EEG record 6).

step, the dipole position vectors used in the clustering are those of the selected windows, i.e. windows with a high S_k and low RRE_k value. Since it was found that the parameter S used in the selection step of the method often obtains its highest values at the wave of the epileptiform events, rather than at the spike, the dipole analysis window of the method is then shifted in time with respect to the analysis window of the definite epileptiform events. This could explain a systematic shift between the epileptiform cluster and the ROD: the shift in position between both could be related to a spreading phenomena of the epileptiform events resulting in different dipole positions obtained for the events at their peak and at their subsequent wave.

3.4. Template

Fig. 6 displays the spatio-temporal template **T** (in red) obtained by the method, superimposed on $\mathbf{V}_{\text{def}}$, the mean of all EEG segments whose dipole position vector lies inside the constructed ROD (in green). In this figure it can be seen that the method returns a template **T** which corresponds well with $\mathbf{V}_{\text{def}}$, hence confirming the validity of the template, except for EEG records 7 and 8. For EEG record 7 the method fails, as already stated, because no epileptiform cluster could be formed, and hence no valid template could be derived. EEG record 8 contains widespread epileptiform activity. Although it was possible to localize the epileptic focus, the retrieved time series are

Table 7
Summary of the detection performance of the different detection methods evaluated using PR-curves

EEG	Mimetic		Wavelet		Dipole analysis		Spatio-temporal	
	Sens	Selc	Sens	Selc	Sens	Selc	Sens	Selc
1	0.79	0.89	0.78	0.76	0.87	0.28	0.85	0.91
2	0.95	0.90	0.80	0.89	0.89	0.15	0.97	0.90
3	1.00	0.82	0.92	0.85	0.92	0.34	0.87	0.80
4	1.00	0.58	0.93	0.74	0.98	0.34	0.96	0.76
5	1.00	0.95	0.94	0.93	0.69	0.28	0.99	0.94
6	0.90	0.64	0.85	0.92	0.90	0.21	0.94	0.93
7	1.00	0.94	0.97	0.94	0.89	0.05	1.00	0.05
8	0.94	0.93	0.59	0.78	0.83	0.15	0.81	0.85
Mean	0.95	0.83	0.85	0.85	0.87	0.23	0.92	0.77

Listed sensitivity (sens) and selectivity (selc) values for the different detection methods are the values obtained with the working point on the PR-curve equal to the point closest to the optimal point (1.00, 1.00). The temporal detection methods were applied to the EEG channel most clearly showing the epileptiform activity. The proposed detection method shows comparable or better detection performance for all EEG records, except 7 and 8.

inaccurate for forming a valid template. For EEG records 2 and 6 we find a relatively high value of RRE. For these EEG records, $\mathbf{V}_{def}$ contains background activity not related to the epileptiform events (channels Fp2-F8 and F8-T4 for EEG record 2, and channel Fp2-F4 for EEG record 6). The template, however, is based on a single dipole model and can only capture the activity on the channels related to the epileptiform activity, as is actually desired.

3.5. Detection performance

Table 7 shows the sensitivity and selectivity values for the different detection methods obtained with the working point on the PR-curve equal to the point M closest to the optimal point (1.00, 1.00).

From Table 7 we can draw a number of conclusions. First, the two temporal detection methods perform reasonably well. Neither clearly outperforms the other: for EEG records 1, 2, 5 and 8 the mimetic based detection method gives better results, for EEG records 4 and 6 the wavelet based detection method performs best, while showing similar performance for EEG records 3 and 7. It is important to note that the temporal methods, as used in this evaluation, require the visual selection of the EEG channel that most clearly shows the epileptiform activity (resulting in the best possible performance obtainable by these methods).

Second, the spatial approach of Van Hoey et al. has a low detection performance and, hence, is not sufficient for the detection of epileptiform events in its own.

Third, when comparing the performance of all methods, we find a comparable or better detection performance of the new method, except for EEG records 7 and 8. This is due to the invalidity of the template, as discussed. Further investigation into the detection results of the proposed method (for all EEG records) reveals that most false positives are due to electrode artifacts. Eye blink artifacts generally caused no problems. Occasionally the method correctly marked an epileptiform event that was not labelled as such by the experts because it was obscured by muscle artifact.

4. Discussion

4.1. Results and methodological considerations

The starting point of the proposed method is a spatial detection method (Van Hoey et al., 2000; Van Hoey, 2000). From the results presented in this study in Section 3.5 it is clear that for spike detection, inclusion of the temporal information is vital to obtain a good detection performance. To be able to make use of this valuable information, an alignment of the dipole series was required. This problem could be solved by aligning the time series at the point of maximal sharpness, as described in, so that all spikes were aligned at their peaks. No prior information regarding the temporal waveform is assumed or implied, only that the epileptiform waveform is characterized by a large sharpness at the peak of the spike. A correct alignment could not be obtained by aligning the dipole time series at the maximum of the time series, because sometimes the wave following the spike was larger in amplitude than the spike itself. The sharpness as calculated here has the same interpretation as in Dingle et al. (1993), but was more conveniently calculated using two linear filter operations, eliminating the need for a wave and halfwaves analysis.

For the dipole analysis we used a simple spherical head model. More complex, realistic head models exist (Heinonen et al., 1997; Hallez et al., 2005). Although the use of a spherical head model introduces localization errors, we preferred this simple head model because it allows the use of an analytic formula for the forward problem (Salu et al., 1990). This is thus not a restriction of the method: if preferred, a realistic head model can be used to obtain more accurate localization results for clinical application (Ebersole and Hawes-Ebersole, 2007). However, for the detection of epileptiform events as performed in the proposed method, we expect the influence of the head model to be of minor importance. Most important is that a meaningful clustering can be obtained. The use of a realistic head model would result in a lower estimation bias and variance on the dipole position estimates. As such, however, the lower bias would only imply a shift of the fitted dipole positions, which is unimportant when forming clusters of dipoles (since all dipoles will shift roughly with the same amount). The smaller variance would only imply that a smaller value of δ_r can be set.

In our study we used the region of definites (ROD) as an estimate of the epileptic focus. The gold standard to determine the epileptic focus is by using depth-electrodes. To fully quantify the localization results of the method, we should thus use a realistic head model in the source analysis step of the method, and compare the results with the position of the focus as determined by a depth-recording. The current setup serves to demonstrate that the method is capable of identifying activity in the EEG useful for automatically determining the position of the epileptic focus. The evaluation of EEG source analysis as a noninvasive examination (e.g., as part of the presurgical evaluation) is outside the scope of this work.

For the calculation of sensitivity and selectivity values of the different detection methods, we used a dichotomous labelling (*definite* and *questionable*) of the epileptiform events, and specified the rules for the construction of the consensus labelling and assignment into TP, FP and FN. We believe that the use of a dichotomous labelling and the specified rules for the construction of the consensus labelling and assignment into TP, FP and FN reflect the true nature and purpose of the detection of epileptiform events: one does not want to miss obvious epileptiform activity and one wants as few spurious detections due to artifacts as possible, but one can tolerate that events, for which no clear consensus between the experts exists, are not detected (missed questionable epileptiform activity is

not penalized due to the rule of not including missed questionable events).

It is difficult to compare the detection performance of the method with the detection performance of methods reported in the literature, since the detection performance is highly dependent on the particular data set used, and no universal EEG data set exists to evaluate (or develop) a detection method (Wilson and Emerson, 2002). Here we chose to implement some other detection methods, apply them to the same data set labeled by two independent experts, and study their performance using PR-curves. We believe that this setup allows us to make statements regarding the performance of the method compared to other methods and view the performance of the proposed method in its proper context.

The proposed method does not contain any special rules to handle artifacts, although this is commonly found in detection methods. The data set we used contained eye blink artifacts, as well as (some) muscle and electrode artifacts. The latter were the source of a number of false positives; eye blink artifacts were in general no cause of false positives. For this data set, a good detection performance could be obtained and clinical relevant information could be derived, without paying special attention to artifacts present. This is partly due to the artifact rejection inherent in the window selection criterion $||\mathbf{r}_k||_2 < \theta_e$ (Flanagan et al., 2003). For other data with contamination of different sources, if necessary, an artifact removal *pre-processing step* can easily be added to the method. Eye blink and electrode artifacts could be removed using an ICA based removal algorithm (Vigario, 1997; Joyce et al., 2004). For muscle artifacts one could opt for the method described in De Clercq et al. (2006).

The proposed method has features in common with the method presented in Ossadtchi et al. (2004). That method searches for significant clusters of dipoles by applying RAP-MUSIC to a signal subspace spanned by ICA components exhibiting spike-like characteristics. For our data set, PCA was sufficient to extract the topography of the epileptiform events and showed good results. Since we explicitly search for windows with a high S value, the dimension of the signal subspace for these windows will be close to one, so that one can deduce that the use of ICA and/or RAP-MUSIC for these windows will not greatly change the results of the source analysis step. ICA and/or RAP-MUSIC, however, might be able to extract useful information from windows that are now excluded because of high background activity (resulting in a lower S value).

4.2. Clinical relevance

The method derives important clinical relevant information from the EEG. It provides information regarding the epileptic focus by presenting the result of the dipole clustering. As such, it gives the location of the epileptic focus, together with the dipole time series. The method allows the identification and quantification of epileptiform events throughout a recording, which is of considerable importance in the diagnosis and characterization of epilepsy.

If desired, the method could also be used as an *offline exploration tool*. Given an EEG record, one could explore the focal activity in this record by changing the parameters that handle the selection of windows, θ_S and θ_{RRE}, and by observing the clusters of dipoles and corresponding time series.

The method first derives a template $\mathbf{T}$ from an EEG record of limited duration (about 20 min, as was the case in this study), which is subsequently used for detection. Once a template has been derived, this template could be used for real-time detection of epileptiform events.

4.3. Limitations

The method as presented here clearly has the limitation that it is restricted to *focal* epileptiform events, since it explicitly searches for a single dominant source with a dipolar field. Thus, it cannot be used for detecting epileptiform events in generalized epilepsy or epilepsy in which there are multiple foci. However, the method could easily be extended within the current framework to relax some of these limitations. For example, instead of building only one template, one could derive a template for each cluster that one considers important or relevant. A selection criterion similar to the one implemented now to determine the epileptiform cluster could be used.

Visual inspection of the EEG is still required to a certain level. However, the method greatly facilitates this process. The selection and clustering procedure is completely automated and inspection of the clustering results only requires a fraction of the time needed for a full visual analysis to determine the epileptiform focus. If the EEG record would contain widespread activity or activity from multiple foci, this should be apparent in the clustering results. For widespread activity clustering results will probably be similar to what was observed in subject 8. For multiple foci we expect to find different clusters showing an epileptiform pattern.

The method was developed based on EEG recordings from eight patients, and tested on the same data set. A leave-one-out cross validation was used to handle the free parameters of the method in order to get a fair estimate of the performance of the method. However, future experiments are needed to confirm the positive findings of the method and to elucidate whether the presented methodology generalizes to data independent from our data set.

References

Acir N, Oztura I, Kuntalp M, Baklan B, Guzelis C. Automatic detection of epileptiform events in EEG by a three-stage procedure based on artificial neural networks. IEEE Trans Biomed Eng 2005;52(1):30–40.

Adjouadi M, Cabrerizo M, Ayala M, Sanchez D, Yaylali I, Jayakar P, et al. Detection of interictal spikes and artifactual data through orthogonal transformations. J Clin Neurophysiol 2005;22(1):53–64.

Adjouadi M, Sanchez D, Cabrerizo M, Ayala M, Jayakar P, Yaylali I, et al. Interictal spike detection using the Walsh transform. IEEE Trans Biomed Eng 2004;51(5):868–72.

Black MA, Jones RD, Carroll GJ, Dingle AA, Donaldson IM, Parkin PJ. Real-time detection of epileptiform activity in the EEG: a blinded clinical trial. Clin Electroencephalongr 2000;31(3):122–30.

De Clercq W, Vergult A, Vanrumste B, Van Paesschen W, Van Huffel S. Canonical correlation analysis applied to remove muscle artifacts from the electroencephalogram. IEEE Trans Biomed Eng 2006;53(12):2583–7.

Dingle AA, Jones RD, Carroll GJ, Fright WR. A multistage system to detect epileptiform activity in the EEG. IEEE Trans Biomed Eng 1993;40(12):1260–8.

Ebersole JS, Hawes-Ebersole S. Clinical application of dipole models in the localization of epileptiform activity. J Clin Neurophysiol 2007;24(2):120–9.

Flanagan D, Agarwal R, Wang YH, Gotman J. Improvement in the performance of automated spike detection using dipole source features for artefact rejection. Clin Neurophysiol 2003;114(1):38–49.

Frost JD. Automatic recognition and characterization of epileptiform discharges in the human EEG. J Clin Neurophysiol 1985;2(3):231–49.

Glover JR, Raghavan N, Ktonas PY, Frost JD. Context-based automated detection of epileptogenic sharp transients in the EEG – elimination of false positives. IEEE Trans Biomed Eng 1989;36(5):519–27.

Goelz H, Jones RD, Bones PJ. Wavelet analysis of transient biomedical signals and its application to detection of epileptiform activity in the EEG. Clin Electroencephalogr 2000;31(4):181–91.

Gotman J, Gloor P. Automatic recognition and quantification of interictal epileptic activity in human scalp EEG. Electroencephalogr Clin Neurophysiol 1976;41(5):513–29.

Hallez H, Vanrumste B, Van Hese P, D'Asseler Y, Lemahieu I, Van de Walle R. A finite difference method with reciprocity used to incorporate anisotropy in electroencephalogram dipole source localization. Phys Med Biol 2005;50(16):3787–806.

Hara J, Musha T, Shankle WR. Approximating dipoles from human EEG activity: the effect of dipole source configuration on dipolarity using single dipole models. IEEE Trans Biomed Eng 1999;46(2):125–9.

Heinonen T, Eskola H, Dastidar P, Laarne P, Malmivuo J. Segmentation of T1 MR scans for reconstruction of resistive head models. Comput Methods Programs Biomed 1997;54(3):173–81.

James CJ, Jones RD, Bones PJ, Carroll GJ. Detection of epileptiform discharges in the EEG by a hybrid system comprising mimetic, self-organized artificial neural network, and fuzzy logic stages. Clin Neurophysiol 1999;110(12):2049–63.

Joyce CA, Gorodnitsky IF, Kutas M. Automatic removal of eye movement and blink artifacts from EEG data using blind component separation. Psychophysiology 2004;41(2):313–25.

Kobayashi K, Akiyama T, Nakahori T, Yoshinaga H, Gotman J. Systematic source estimation of spikes by a combination of independent component analysis and RAP-MUSIC. I. Principles and simulation study. Clin Neurophysiol 2002;113(5):713–24.

Latka M, Was Z, Kozik A, West BJ. Wavelet analysis of epileptic spikes. Phys Rev E 2003;67(5):052902.

Liu HS, Zhang T, Yang FS. A multistage, multimethod approach for automatic detection and classification of epileptiform EEG. IEEE Trans Biomed Eng 2002;49(12):1557–66.

Nelder JA, Mead R. A simplex method for function minimization. Comput J 1965;7:308–13.

Oostendorp TF, Delbeke J, Stegeman DF. The conductivity of the human skull: Results of in vivo and in vitro measurements. IEEE Trans Biomed Eng 2000;47(11):1487–92.

Ossadtchi A, Baillet S, Mosher JC, Thyerlei D, Sutherling W, Leahy RM. Automated interictal spike detection and source localization in magnetoencephalography using independent components analysis and spatio-temporal clustering. Clin Neurophysiol 2004;115(3):508–22.

Salu Y, Cohen LG, Rose D, Sato S, Kufta C, Hallett M. An improved method for localizing electric brain dipoles. IEEE Trans Biomed Eng 1990;37(7):699–705.

Theodoridis S, Koutroumbas K. Pattern recognition. New York: Academic Press; 1999.

Tzallas AT, Karvelis PS, Katsis CD, Fotiadis DI, Giannopoulos S, Konitsiotis S. A method for classification of transient events in EEG recordings: application to epilepsy diagnosis. Methods Inform Med 2006;45(6):610–21.

Van Hoey G. Detectie en bronlokalisatie van epileptische hersenactiviteit met behulp van EEG-signalen. Ph.D. Thesis, Ghent University, Belgium; 2000 [in Dutch].

Van Hoey G, Vanrumste B, Van de Walle R, Boon P, Lemahieu I, D'Havé, M et al. Detection and localization of epileptic brain activity using an artificial neural network for dipole source analysis. In: Proceedings of the EUSIPCO2000 conference, September 5–8, 2000, Tampere, Finland.

Van Veen BD, Buckley KM. Beamforming: a versatile approach to spatial filtering. IEEE Acoust Speech Signal Process Mag 1988;5:4–24.

Vanrumste B, Jones RD, Bones PJ, Carroll GJ. Slow-wave activity arising from the same area as epileptiform activity in the EEG of paediatric patients with focal epilepsy. Clin Neurophysiol 2005;116(1):9–17.

Vigario RN. Extraction of ocular artefacts from EEG using independent component analysis. Electroencephalogr Clin Neurophysiol 1997;103(3):395–404.

Wilson SB, Emerson R. Spike detection: a review and comparison of algorithms. Clin Neurophysiol 2002;113(12):1873–81.

Wilson SB, Harner RN, Duffy FH, Tharp BR, Nuwer MR, Sperling MR. Spike detection. 1. Correlation and reliability of human experts. Electroencephalogr Clin Neurophysiol 1996;98(3):186–98.